

result of Ref. 34. Thus it does not appear that the effect at 980 MeV observed in our data is wholly kinematic in origin. Additional evidence against this type of kinematical interpretation has been given recently.^{36,37}

D. Final States $\Sigma^-(1385)\eta$ and $\Sigma^-(1610)\eta$

Events with the π^-A effective mass squared lying between 1.80 and 2.10 GeV^2 were taken as being representative of the $\Sigma^-(1385)$ production. Taking the background into account, it was estimated that about 25% of these events did not correspond to $\Sigma^-(1385)$ production. The four-momentum-transfer distribution is shown in Fig. 28(a). The production process appears to be peripheral.

³⁶ V. E. Barnes, S. U. Chung, R. L. Eisner, E. Flaminio, P. Guidoni, J. B. Kinson, N. P. Samios, D. Bassano, M. Goldberg, and K. Jaeger, *Phys. Rev. Letters* **23**, 610 (1969).

³⁷ J. Mott, paper presented at the meeting of the division of particles and fields, Boulder, Colo. 1969 (unpublished).

Events with the π^-A effective mass squared lying between 2.4 and 2.8 GeV^2 were taken as being representative of the $\Sigma^-(1610)$ production. Taking into account the background, it was estimated that about 60% of these events did not correspond to $\Sigma^-(1610)$ production. The four-momentum transfer distribution is shown in Fig. 28(b). This reaction is not as peripheral as the reaction $K^-n \rightarrow \eta\Sigma^-(1385)$.

ACKNOWLEDGMENTS

We would like to express our gratitude to the operating personnel of the bubble chamber and the staff of Argonne National Laboratory, particularly Dr. M. Derrick, Dr. L. Voyvodic, and Dr. F. Schweingruber, for their help. We would also like to thank the scanning and measuring crew for their cooperation and care in the film analysis.

Coherent Production of the $K^-\pi^+\pi^-$ System in K^-d Interactions at 5.5 GeV/c^\dagger

B. WERNER,* R. AMMAR,† R. E. P. DAVIS, W. KROPAC,‡ AND H. YARGER†

Northwestern University, Evanston, Illinois 60201

AND

Y. CHO, M. DERRICK, B. MUSGRAVE, J. J. PHELAN,§ AND T. P. WANGLER

Argonne National Laboratory, Argonne, Illinois 60439

(Received 7 July 1969)

K^-d interactions were studied at an incident momentum of 5.5 GeV/c in a 5-eV/ μb exposure of the 30-in. deuterium bubble chamber at the Argonne Zero-Gradient Synchrotron. The dominant feature of the reaction $K^-d \rightarrow K^-\pi^+\pi^-d$ is $\bar{K}^*(890)$ production, although the low-mass enhancement, usually referred to as d^* , is also prominent in the $d\pi^-$ mass spectrum. The low momentum transfer to the deuteron imposed by coherent production strongly favors a $K\pi\pi$ mass in the region of the Q enhancement. As is usually observed, the production and decay characteristics of the $K\pi\pi$ system are generally compatible with a 1^+ spin-parity assignment. A study of the $K^-\pi^+$ system reveals an s -wave- p -wave interference similar to that observed in $K\pi$ scattering. The data are compared with the predictions of a double-Regge-pole model.

I. INTRODUCTION

THE results reported in this paper were obtained from a 370 000-picture exposure of the 30-in. deuterium bubble chamber to an electrostatically separated, high-purity beam¹ of 5.5- GeV/c negative

kaons produced at the Argonne Zero-Gradient Synchrotron (ZGS). The experimental arrangement was identical to that used in a previous study of K^-p interactions at this energy.² We have analyzed those four-prong events with at least one stopping positive track which is either a proton or a deuteron and studied the reaction

$$K^-d \rightarrow K^-\pi^+\pi^-d. \quad (1.1)$$

Coherent $K\pi\pi$ production has been studied at other energies using both incident K^+ and K^- mesons.³⁻⁶ At 5.5 GeV/c the kinematics of coherent production

† Work supported by U. S. Atomic Energy Commission and the National Science Foundation.

* This work forms part of a dissertation to be submitted to the Department of Physics, Northwestern University, in partial fulfillment of the requirements for the Ph.D. degree.

‡ Present address: Department of Physics, University of Kansas, Lawrence, Kan. 66044.

§ Now at the Rutherford Laboratory, Chilton, Didcot, Berkshire, England.

¹ T. H. Fields *et al.*, Argonne National Laboratory Report No. THF/ELG/UEK-1, 1961 (unpublished); R. Ammar *et al.*, in Proceedings of the 1966 International Conference on Instrumentation for High-Energy Physics, Stanford-USAEC Report No. 660918, p. 620 (unpublished).

² F. Schweingruber *et al.*, *Phys. Rev.* **166**, 1317 (1968).

³ I. Butterworth *et al.*, *Phys. Rev. Letters* **15**, 500 (1965).

⁴ D. Denegri *et al.*, *Phys. Rev. Letters* **20**, 1194 (1968).

⁵ W. Hoogland *et al.*, *Nucl. Phys.* **B11**, 309 (1969).

⁶ K. Buchner *et al.*, *Nucl. Phys.* **B9**, 286 (1969).

strongly inhibits the production of $K^-\pi^+\pi^-$ systems with mass greater than about 1.6 GeV. In our data a broad enhancement, commonly called the Q , dominates the $K\pi\pi$ system where we define the Q to be the mass range 1.1–1.5 GeV. There is no evidence in our data for any structure in the Q enhancement as suggested by some other groups.^{7,8} Analysis of the decay angular distributions of $\bar{K}^*\pi$ events in the Q region agrees with the $J^P=1^+$ assignment observed previously.⁹ At our energy, reaction (1.1) shows almost pure $\bar{K}^*(890)$ production. In addition, an enhancement is observed in the $d\pi^-$ mass spectrum at a mass of 2200 MeV and there is also some ρ^0 production.

The distribution of the polar decay angle θ of the $\bar{K}^*(890)$ with respect to the incident beam shows a pronounced $\cos^2\theta$ dependence with a strong forward-backward asymmetry. A spherical harmonic moment analysis of this angular distribution as a function of $K^-\pi^+$ mass yields results in striking agreement with those from the reaction $K^+p \rightarrow \Delta^{++}K^+\pi^-$,¹⁰ which is believed to proceed via one-pion exchange (OPE). This similarity could be expected if Q production proceeds mainly via a "Deck"-type¹¹ mechanism where the K^- dissociates into $\bar{K}^*\pi^-$ with subsequent diffractive scattering of the π^- off the deuteron. A Reggeized version of this model¹² accounts for the main features of these results.

II. EXPERIMENTAL DETAILS

A. Exposure and Analysis

The exposure represents 1.32×10^8 cm of K^- track length corresponding to a cross-section basis of 5.2 eV/ μ b. The beam momentum determined by fitting τ decays was found to be 5.52 GeV/ c with a full width of 0.10 GeV/ c .

The film was scanned for events of the four-prong topology with one of the positive tracks stopping and having an ionization consistent with being either a proton or a deuteron. This yielded 11 500 events. A second scan has been completed on 25% of the film to determine scanning efficiency and possible scanning bias.

A major systematic scanning bias exists for events having the square of the momentum transfer to the deuteron less than 0.02 (GeV/ c)². This results in a deuteron of range less than 1 mm and, as a result, these events were not likely to have been classified as four-pronged events. This is consistent with the apparent turnover in the distribution for t' shown in Fig. 1,

⁷ B. Bassompierre *et al.*, Nuovo Cimento **49A**, 373 (1967).

⁸ G. Goldhaber *et al.*, Phys. Rev. Letters **19**, 972 (1967).

⁹ J. C. Park and S. Kim, Phys. Rev. **174**, 2165 (1968); C. Y. Chien *et al.*, Phys. Letters **28B**, 143 (1968).

¹⁰ P. Schlein, in *Proceedings of the Informal Conference on Meson Spectroscopy, University of Pennsylvania, 1968* (W. A. Benjamin, Inc., New York, 1968); T. G. Trippe *et al.*, Phys. Letters **28B**, 203 (1968).

¹¹ R. Deck, Phys. Rev. Letters **13**, 169 (1964).

¹² E. L. Berger, Phys. Rev. **166**, 1525 (1968).

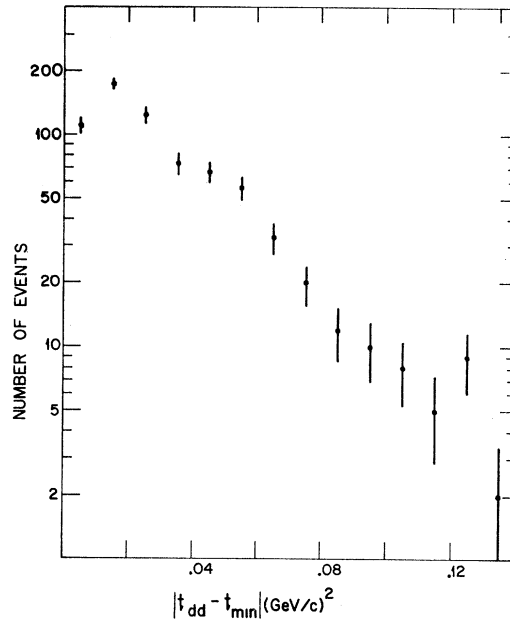


FIG. 1. Distribution in four-momentum transfer squared to the deuteron $|t'_{dd} - t'_{min}|$, for events assigned to the reaction $K^-d \rightarrow K^-\pi^+\pi^-d$.

where $t' = t'_{dd} - t'_{min}$. An extrapolation to the kinematic limit using the function $e^{-At'}$ predicts a 17% loss of events due to this effect.

The geometrical reconstruction and fitting of events was done using the ANL TVGP-GRIND system of programs.¹³ Events found in the first scan which failed in the reconstruction program were remeasured. Finally, 91% of the sample gave a satisfactory geometrical reconstruction. After kinematic fitting, all events were checked on the scan table by physicists for consistency of the track ionizations with those expected from the kinematic fit.

Quoted cross sections are based on the total length of K^- beam track estimated from a beam track count, corrected for beam contamination, which was measured to be less than 5%. In addition, corrections were made for scanning efficiency, losses in reconstruction, and the effect of the χ^2 probability cut used to increase the purity of the coherent sample.

B. Selection of Events

Almost 86% of the events fitting reaction (1.1) also gave kinematic fits to

$$K^-d \rightarrow K^-\pi^+\pi^-pn. \quad (2.1)$$

Correlations between the fitted momenta (2.1) of the proton and neutron can be used to show that most events which fit both reactions (1.1) and (2.1) really are events of reaction (1.1). An event belonging to reaction (1.1) should easily fit reaction (2.1) since a

¹³ Descriptive accounts of these programs may be obtained from the High-Energy Physics Program Library, Argonne National Laboratory, Argonne, Ill. 60439.

deuteron is almost kinematically equivalent to a proton and a neutron traveling in the same direction with small relative momentum. Thus, if the ambiguous event is really an event of reaction (1.1), the hypothesized neutron and proton momenta should be collinear. The distribution of the cosine of the angle between the neutron and proton momentum for all events fitting hypothesis (2.1) is shown in Fig. 2(a). Those events giving a kinematic fit to both reactions (1.1) and (2.1) are shaded and have a very pronounced tendency to be collinear. Events which fit only reaction (2.1) show an isotropic distribution in this angle in accordance with the spectator model.¹⁴

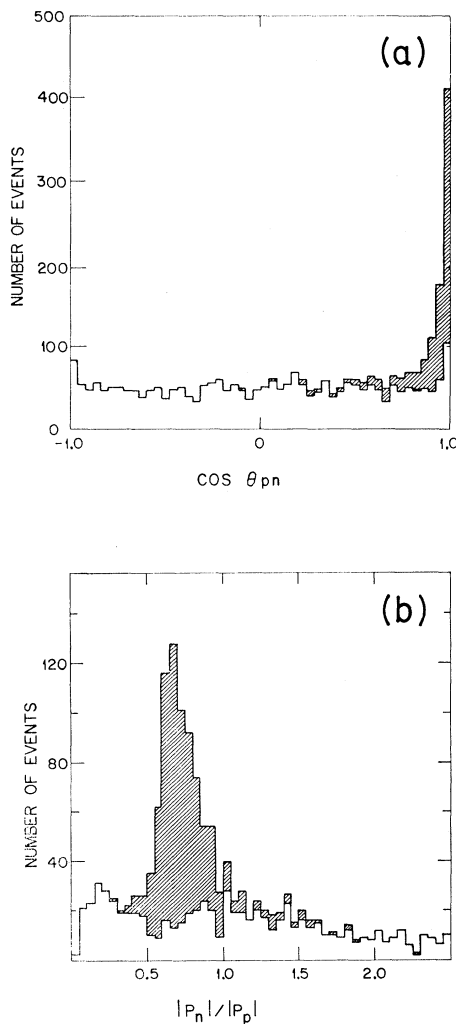


FIG. 2. (a) Cosine of the angle between the fitted proton and neutron vector momenta for events fitting the reaction $K^-d \rightarrow K^-n\pi^+\pi^-(p)$. Events also fitting the reaction $K^-d \rightarrow K^-d\pi^+\pi^-$ are shown shaded. (b) Distribution of the ratio between the magnitudes of the fitted neutron and proton momenta for events fitting the reaction $K^-d \rightarrow K^-n\pi^+\pi^-(p)$. Events also fitting the reaction $K^-d \rightarrow K^-d\pi^+\pi^-$ are shaded.

¹⁴ P. Fleury, *Methods In Sub-Nuclear Physics*, (Gordon and Breach, Science Publishers, Inc., New York, 1967), Vol. 2, p. 560.

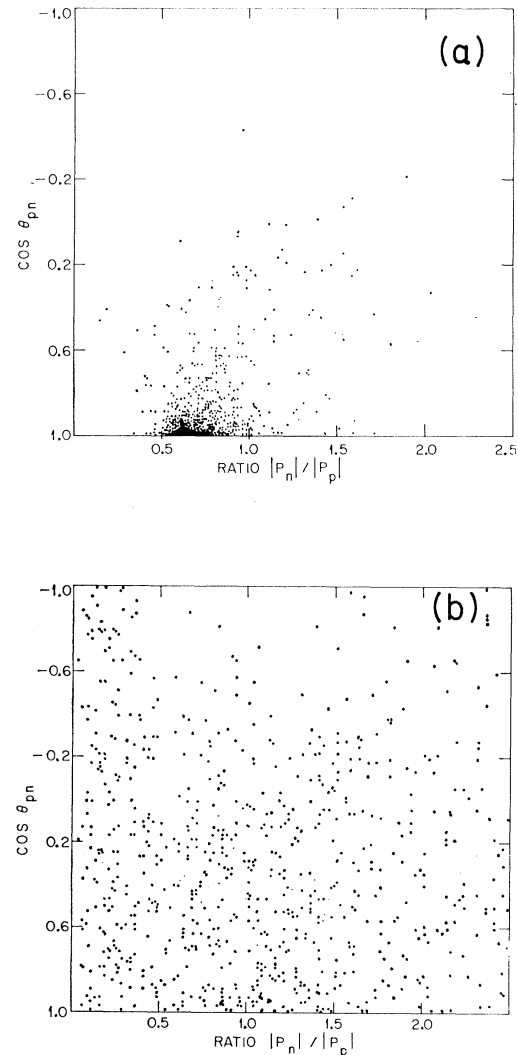


FIG. 3. (a) Scatter diagram for events fitting both the reactions $K^-d \rightarrow K^-d\pi^+\pi^-$ and $K^-d \rightarrow K^-n\pi^+\pi^-(p)$. The cosine of the proton-neutron angle is plotted versus the ratio of their fitted momenta. (b) Scatter diagram for events only fitting the reaction $K^-d \rightarrow K^-n\pi^+\pi^-(p)$. The cosine of the proton-neutron angle is plotted versus the ratio of their fitted momenta.

Often the stopping track is short and its momentum can only be determined by a range measurement. If the track is really a deuteron but is interpreted as a proton, with the difference in momentum taken away by a neutron, the ratio of the magnitude of neutron to proton momentum is determined from the range-energy relations to be about 0.67. The distribution of this ratio for events fitting reaction (2.1) is shown in Fig. 2(b). Events fitting both hypotheses (1.1) and (2.1), are shown shaded and have a tendency to be clustered about the value 0.67 as expected if they represent (1.1). This provides additional support for their assignment to reaction (1.1).

The two preceding tests are combined in Fig. 3(a), where we interpret the obvious clustering as due to

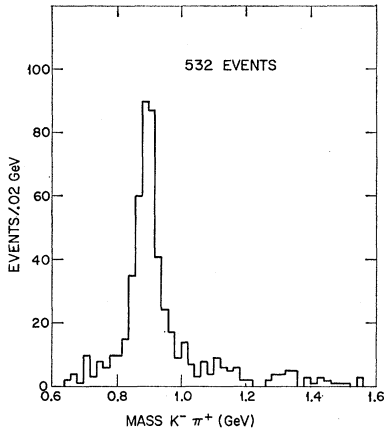


FIG. 4. Effective mass distribution for the $K^-\pi^+$ combination from those events having no K^-/π^- ambiguity in fitting the hypothesis $K^-d \rightarrow K^-d\pi^+\pi^-$.

genuine deuteron events. The smearing out of this cluster arises primarily from events having a stopping track with a range of less than 0.5 cm which are often poorly measured. Events giving a fit to reaction (2.1) and not to reaction (1.1) exhibit a rather uniform distribution on such a scatter plot as seen in Fig. 3(b). This figure also indicates that few events which belong to reaction (1.1) are being fitted only to reaction (2.1) by GRIND.

Finally, we selected as genuine only those fits to (1.1) which have a χ^2 probability greater than 1%, since those with a χ^2 probability of less than 1% were found to be less likely to satisfy the criteria discussed above. In so doing, we optimized the purity of our sample without too seriously affecting the number of events or introducing any experimental bias against low-momentum deuterons. Approximately 26% of these events gave two kinematical fits in which the K^- and π^- choice for the two negative tracks was permuted. This K^-/π^- ambiguity was resolved by noting that

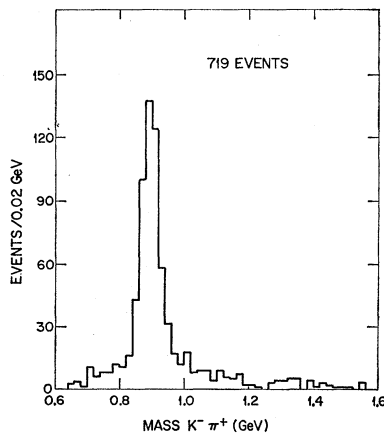


FIG. 5. Effective mass distribution for the $K^-\pi^+$ combination from events assigned to the reaction $K^-d \rightarrow K^-d\pi^+\pi^-$.

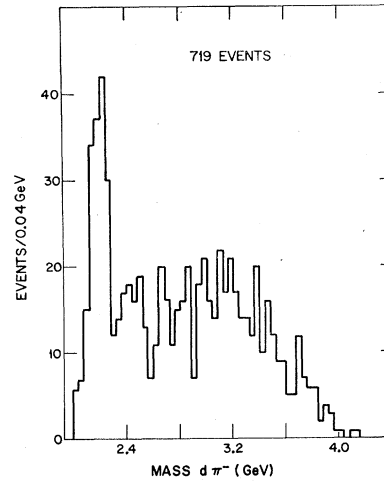


FIG. 6. Effective mass distribution for the $d\pi^-$ combination in the reaction $K^-d \rightarrow K^-d\pi^+\pi^-$.

the $K^-\pi^+$ mass spectrum for events in which there is no K^-/π^- ambiguity is consistent with almost pure $\bar{K}^*(890)$ production as shown in Fig. 4. This suggests that fits with a $K^-\pi^+$ mass combination near 890 MeV were more likely to be genuine. Thus ambiguities for which at least one $K^-\pi^+$ mass combination was within 50 MeV of 890 MeV were resolved by selecting the fit which gave the $K^-\pi^+$ mass closest to 890 MeV. Otherwise, the fit having the largest χ^2 probability was chosen. After resolving the K^-/π^- ambiguity in this manner, the characteristics of the ambiguous and unambiguous events were compared and found to be consistent.

The cross section for reaction (1.1) obtained using events with a visible deuteron is given in Table I. A cross section corrected for loss of events with an unseen deuteron is also given.

III. RESONANCE PRODUCTION

A. $\bar{K}^*(890)$

The $K^-\pi^+$ mass spectrum for events belonging to reaction (1.1), shown in Fig. 5, indicates almost all the $K^-\pi^+$ combinations are associated with $\bar{K}^*(890)$. The

TABLE I. Cross sections.^a

Final state	Cross section (μb)
$K^-\pi^-\pi^+d$ (visible deuteron)	194 ± 30
$K^-\pi^-\pi^+d$ (corrected for unseen deuteron)	228 ± 35
$K^-\pi^+d^*$	28 ± 10
Qd \swarrow $\bar{K}^{*0}\pi^-$ (corrected for unseen deuteron)	130 ± 20

^a In defining the cross sections, the \bar{K}^* , d^{*0} , and Q are defined by the mass ranges $0.8 \leq M(K^-\pi^+) \leq 1.0$, $M(d\pi^-) \leq 2.28$, and $1.1 \leq M(\bar{K}^{*0}\pi^-) \leq 1.5$ GeV.

mass and width of the $\bar{K}^*(890)$ for those events having no $K^- \pi^-$ ambiguity¹⁵ were found to be 895 and 58 MeV, respectively.

B. $d\pi$ Enhancements

The $d\pi^-$ mass spectrum of Fig. 6 shows a pronounced enhancement at a mass of 2200 MeV. This peak, usually referred to as d^* ,¹⁶ is simultaneously produced with a $\bar{K}^{*0}(890)$ (Fig. 7). The d^* enhancement is believed to be a $d\pi$ scattering effect resulting from a process in which an exchanged π^- forms a $\Delta(1236)$ resonance with the nucleon, which decays in such a way as to allow recombination of the neutron and proton as shown in Fig. 8.¹⁷ Figure 9 shows the distribution of the $d\pi^-$ scattering angle, which is very sharply forward-peaked, indicating that the deuteron

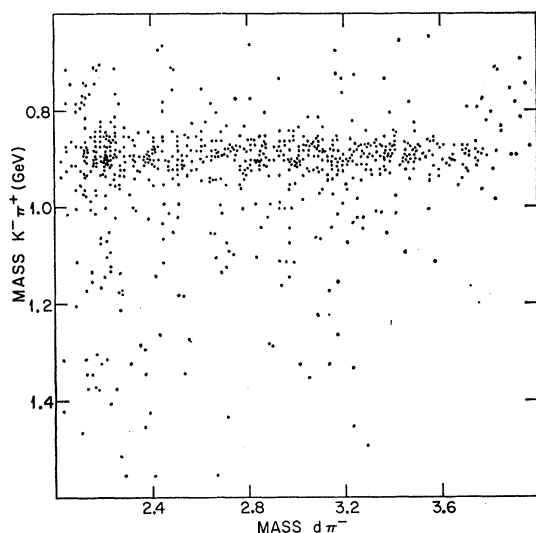


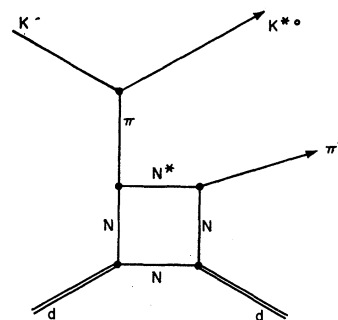
FIG. 7. Scatter diagram showing the $K^- \pi^+$ versus the $d\pi^-$ effective masses for the reaction $K^- d \rightarrow K^- d \pi^+ \pi^-$.

maintains its direction. This implies the interference of many partial waves of high orbital angular momentum and thus excludes the hypothesis that the d^* mass enhancement is the result of a $d\pi^-$ state of definite spin and parity. The polar decay angle distribution of the $\bar{K}^{*0}(890)$ with respect to the beam, not shown, exhibits the alignment expected for a OPE mechanism. Further evidence for a OPE production mechanism is seen in the dependence of the cross section for $K^- d \rightarrow K^- \pi^+ d^*$ as a function of incident beam momentum, which is known to fall off rapidly with beam momentum in a

¹⁵ Only those events were used which do not have a K^-/π^- ambiguity. The method of selecting between the two fits to reaction (1.1) for events having a K^-/π^- ambiguity could bias the $K^- \pi^+$ mass spectrum. Various decay angular distributions were compared for the K^-/π^- ambiguous and unambiguous events and found to be statistically consistent with one another.

¹⁶ M. A. Abolins *et al.*, Phys. Rev. Letters **15**, 125 (1965); A. Forino *et al.*, Phys. Letters **19**, 68 (1965).

¹⁷ B. Eisenstein and H. Gordon, University of Illinois Report No. C00-119S-155 (unpublished).



FEYNMAN DIAGRAM FOR d^{**} PRODUCTION

FIG. 8. Feynman diagram indicating a possible production mechanism for the d^{*0} enhancement.

manner consistent with that expected for OPE processes.¹⁸ Finally, the fact that the d^* mass ~ 2200 MeV is in rough agreement with the sum of the masses of the nucleon and the Δ , while its width (150 MeV) is about that of the Δ , gives additional support for the d^* production mechanism mentioned above. The cross section for the reaction $K^- d \rightarrow \bar{K}^{*0}(890) d^*(2240)$ is shown in Table I.

The $d\pi^+$ mass spectrum, shown in Fig. 10, shows evidence for some d^{*++} production. However, as shown in Sec. IV, the reflection of the $\bar{K}^*(890)$ decay also produces peaking at small and at large $d\pi^+$ masses (see Fig. 25).

C. $K^- \pi^+ \pi^-$ System

The $K^- \pi^+ \pi^-$ mass spectrum of Fig. 11 shows a single broad enhancement within which there is no statistically significant structure. Low momentum transfer to the deuteron, in accordance with the deuteron form factor,¹⁹

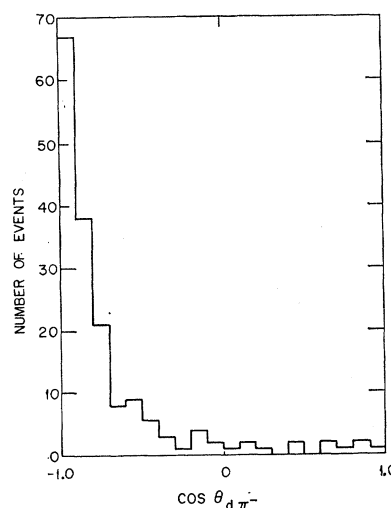


FIG. 9. Polar angular distribution of the π^- , in the $d\pi^-$ rest frame, for events having an effective $d\pi^-$ mass less than 2.28 GeV. The angle is further defined in Fig. 15.

¹⁸ R. Huson (private communication).

¹⁹ M. Gourdin and A. Martin, Nuovo Cimento **11**, 670 (1959).

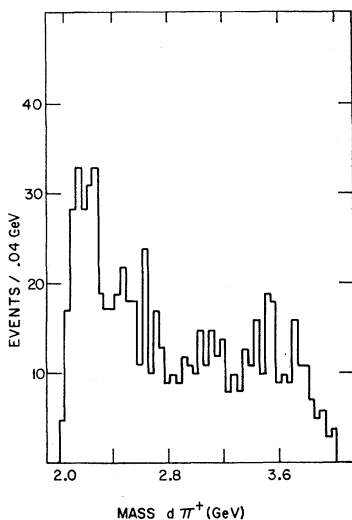


FIG. 10. Effective mass distribution for the $d\pi^+$ combination from events representing the reaction $K^-d \rightarrow K^-d\pi^+\pi^-$.

is required to keep the loosely bound deuteron intact and results in the falloff of the $K\pi\pi$ mass spectrum above 1.6 GeV. The Chew-Low plot of the $K\pi\pi$ system in Fig. 12 shows the extreme peripherality of the reaction. Few events occur in which the square of the momentum transfer to the deuteron is greater than 0.1 $(\text{GeV}/c)^2$, and therefore, because of the kinematic boundary of Fig. 12, heavier $K\pi\pi$ systems such as the L meson, which has been observed in the coherent reaction at higher energy,⁴ are not seen at our energy.

In $K^\pm p$ data at intermediate energies, the Q enhancement is complicated by the presence of $K^*(1420)$ events that decay into $K^\pm\pi^+\pi^-$. Only isoscalar exchange

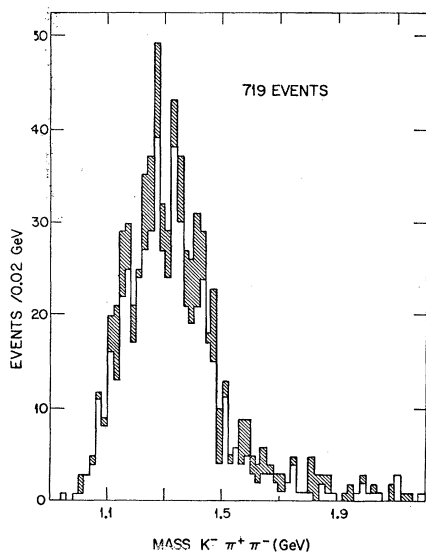


FIG. 11. $K\pi\pi$ effective mass distribution for the reaction $K^-d \rightarrow K^-\pi^+\pi^-d$. Those events for which the $d\pi^-$ mass is less than 2.28 GeV are shown shaded.

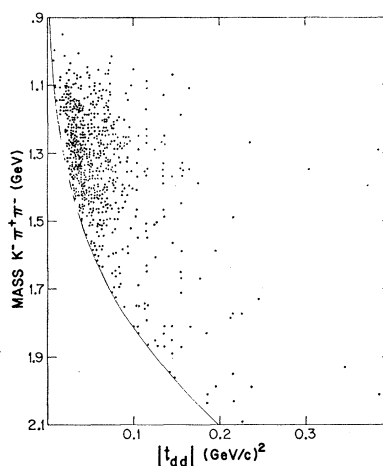


FIG. 12. Chew-Low plot for the reaction $K^-d \rightarrow K^-d\pi^+\pi^-$.

is allowed in the coherent production of the $K\pi\pi$ system. This is expected to inhibit the coherent production of the $K^*(1420)$ meson, as is observed in the reaction $K^-d \rightarrow \bar{K}^0\pi^-d$ at 4.6 GeV/c .²⁰ These data would

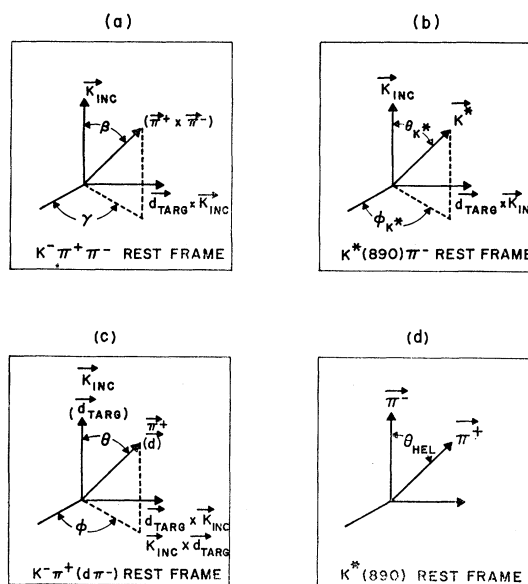


FIG. 13. Definitions of the right-handed reference frames, used for the various angular distributions considered, are as follows: (a) The $K\pi\pi$ system is described by angles β and γ for the $K\pi\pi$ decay plane normal in the $K\pi\pi$ rest frame, where the Z axis is parallel to the direction of the incoming kaon and the Y axis is perpendicular to the $K\pi\pi$ production plane. (b) The two-body decay of the $K\pi\pi$ system into $K^*(890)\pi$ is described by the angles θ_{K^*} and Φ_{K^*} for the π^- defined with respect to the reference frame of case (a). (c) The $K^*(890)$ (d^*) decay is described by the angles θ , Φ of the decay π defined in the K^* (d^*) rest frame with the Z axis parallel to the incoming kaon (deuteron) and the Y axis perpendicular to the plane containing the incident kaon (deuteron) and K^* (d^*). (d) The helicity angle θ_H of the $K^*(890)$ from the decay of the $K\pi\pi$ system is defined in the K^* rest frame using the direction of the odd pion in the $K\pi\pi$ rest frame as Z axis.

²⁰ R. L. Eisner *et al.*, Phys. Letters **28B**, 356 (1968).

TABLE II. $\bar{K}^*(890)\pi$ spin-density matrix elements.^a

$\bar{K}^{*0}\pi^-$ mass (GeV)	No. of events	ρ_{00}	$\text{Re}(\rho_{1-1})$	$\text{Re}(\rho_{10})$
1.1-1.5	378	0.73 ± 0.07	0.02 ± 0.05	0.02 ± 0.03
1.1-1.2	87	0.65 ± 0.14	0.12 ± 0.10	0.03 ± 0.07
1.2-1.3	121	0.72 ± 0.12	0.04 ± 0.08	0.03 ± 0.05
1.3-1.4	109	0.81 ± 0.12	0.05 ± 0.09	0.01 ± 0.06
1.4-1.5	61	0.70 ± 0.15	-0.07 ± 0.12	0.06 ± 0.08

^a The numbers are calculated assuming a $J^P = 1^+$ $K^*\pi$ system and are shown for various intervals of $K^*\pi$ mass. The K^* is defined by the mass range $0.8 \leq M(K^-\pi^+) \leq 1.0$ GeV. The d^{*0} is excluded.

indicate negligible contamination from the $\bar{K}^*(1420)$ in our experiment.

As previously noted, there is a scanning bias for events with a momentum transfer squared to the deuteron of less than 0.02 (GeV/c)², and this selectively removes events from the sample that have a $K^-\pi^+\pi^-$ mass of less than 1250 MeV. Events having an associated d^{*0} are shown shaded. Removal of d^{*0} events from the $K^-\pi^+\pi^-$ mass spectrum does not significantly alter its shape.

Several spin-parity analyses of the low-mass $K\pi\pi$ system⁹ have shown that the Q enhancement is most consistent with a spin-parity assignment of 1^+ . Our data are also quite consistent with a $\bar{K}^*\pi$ system having $J^P = 1^+$ such as might be produced diffractively by Pomernchuk exchange. The angles usually used to illustrate this characteristic are defined in Fig. 13. All decay angular distributions were analyzed by calculating the moments of the spherical harmonics required to describe them. A 1^+ $K\pi\pi$ system produced with spin perpendicular to the beam direction should result in a $\sin^2\beta$ distribution in the polar angle β of the decay plane normal.²¹ Figure 14 shows that the distribution in this angle is dominantly $\sin^2\beta$, while the azimuthal angular distribution has the expected isotropic character. Assuming $J^P = 1^+$, the density-matrix elements shown in Table II were determined for the Q region. The pronounced alignment is indicated by the large value of ρ_{00} , which does not vary over the whole Q mass range.

The lowest orbital angular momentum state for a $K^{*0}\pi$ system with $J^P = 1^+$ is s -wave, which should result in isotropic polar and azimuthal angular distributions. The distribution in these angles for the $\bar{K}^*\pi^-$ system are shown in Fig. 15. The polar angular distribution is

TABLE III. Spin-density matrix elements for the $\bar{K}^*(890)$.^a

$\bar{K}^{*0}\pi^-$ mass (GeV)	No. of events	ρ_{00}	$\text{Re}(\rho_{1-1})$	$\text{Re}(\rho_{10})$
1.1-1.5	378	0.88 ± 0.04	0.01 ± 0.02	0.03 ± 0.03
1.1-1.2	87	0.85 ± 0.08	0.07 ± 0.06	0.09 ± 0.05
1.2-1.3	121	0.83 ± 0.07	-0.03 ± 0.04	0.02 ± 0.05
1.3-1.4	109	1.00 ± 0.07	-0.02 ± 0.04	0.05 ± 0.05
1.4-1.5	61	0.81 ± 0.10	0.05 ± 0.06	0.04 ± 0.06

^a The reference frame is defined in Fig. 17 and the K^{*0} is defined by the mass selection $0.8 \leq M(K^-\pi^+) \leq 1.0$ GeV. The d^{*0} is excluded.

²¹ S. M. Berman and M. Jacob, Phys. Rev. **139**, B1023 (1965).

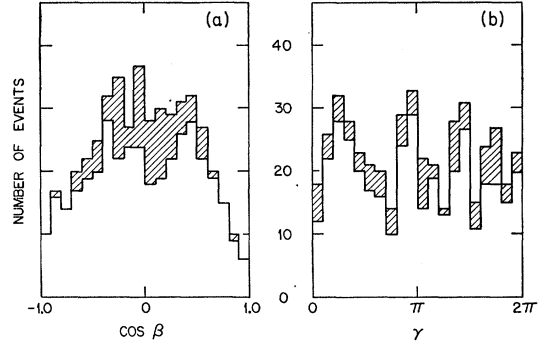


FIG. 14. Polar and azimuthal angular distributions of the $K\pi\pi$ -decay plane normal for events having $K^-\pi^+$ mass between 0.8 and 1.0 GeV and $K^-\pi^+\pi^-$ mass between 1.1 and 1.5 GeV. The beam direction in the $K\pi\pi$ rest frame is used as quantization axis. See also Fig. 13. Events having $d\pi^-$ mass < 2.28 GeV are cross-hatched.

seen to be biased due to the d^{*0} enhancement. Since the outgoing deuteron tends to travel antiparallel to the beam in the c.m. of the reaction, events for which the π^- is emitted backwards with respect to the beam direction in the $\bar{K}^*\pi^-$ rest frame have a low $d\pi^-$ mass appropriate to the d^{*0} . As indicated in Fig. 15, such events show up strikingly near $\cos\theta_{K^*} = 1$. Considering only those events with $\cos\theta_{K^*} < 0.4$, this distribution is clearly inconsistent with the $1+3 \cos^2\theta_{K^*}$ distribution associated with a diffractively produced $2^- \bar{K}^*\pi$ system. The isotropic component of this angular distribution is large, suggesting the dominance of an s -wave $\bar{K}^*\pi$ system.

Finally, we note that the $\bar{K}^*(890)$ decay shows the pronounced alignment with respect to the beam direction expected for a diffractively produced s -wave $\bar{K}^*\pi$ system. This should result in a Y_1^0 orbital state for the $K^-\pi^+$ system. The distributions of the polar and azimuthal angles for the decay of the $\bar{K}^*(890)$ into $K^-\pi^+$ are shown in Fig. 16. Again, the density-matrix elements are substantially independent of $K\pi\pi$ mass, as shown in Table III.

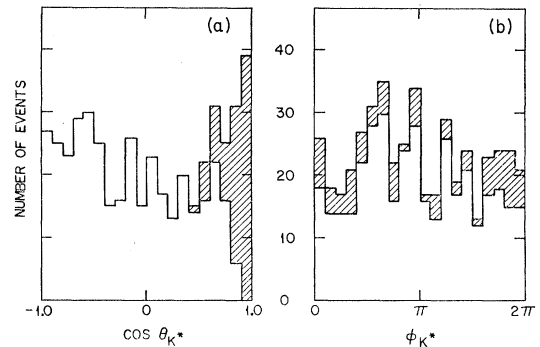


FIG. 15. Polar and azimuthal angular distributions for the $\bar{K}^*(890)\pi^-$ system for events having $K^-\pi^+$ mass between 0.8 and 1.0 GeV and $K^-\pi^+\pi^-$ mass between 1.1 and 1.5 GeV. The beam direction is used as axis of quantization in the $\bar{K}^*\pi^-$ rest frame. See also Fig. 13. Events having $d\pi^-$ mass < 2.28 GeV are cross-hatched.

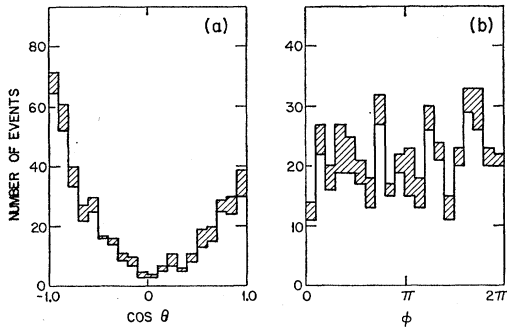


FIG. 16. Polar and azimuthal angular distributions of the $\bar{K}^*(890)$ decay for events having $K^-\pi^+$ mass between 0.8 and 1.0 GeV and $K^-\pi^+\pi^-$ mass between 1.1 and 1.5 GeV. The beam direction is used as quantization axis in the $\bar{K}^*(890)$ rest frame. See also Fig. 13.

The distribution of the $\bar{K}^*(890)$ polar decay angle also shows a marked forward-backward asymmetry with an excess of kaons in the forward direction. This asymmetry appears to be generally observed in other reactions in which a neutral $K^*(890)$ of either strangeness is produced. A considerable amount of data now exists for the reactions $K^-\rho \rightarrow \bar{K}^{*0}(890)n$ and $K^+\rho \rightarrow \bar{K}^{*0}(890)\Delta^{++}$, which are believed to proceed via OPE and both of which show such an effect. In order to study $K\pi$ scattering in the reaction $K^+\rho \rightarrow K^+\pi^-\Delta^{++}$ at 7.3 GeV/c, moments of the $K^+\pi^-$ system were determined as a function of $K^+\pi^-$ mass.¹⁰ These distributions were interpreted by the authors as indicative of the p -wave $K^*(890)$ resonance and an $I=\frac{1}{2}$ $K\pi$ s -wave phase shift which increased slowly from threshold, to reach 90° at around 1100 MeV. We have performed a similar analysis for our data in reaction (1.1) and the $K^-\pi^+$ mass dependence for these moments is shown in

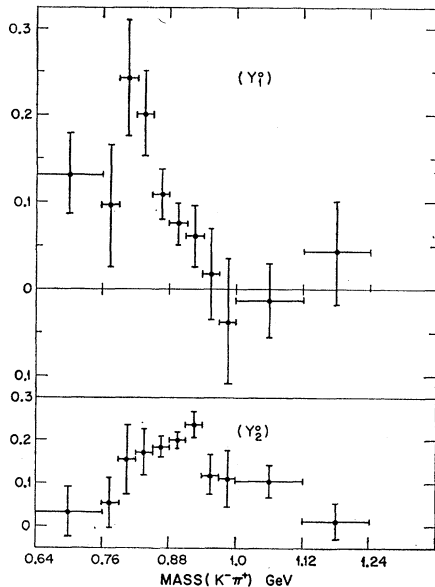


FIG. 17. Variation with $K^-\pi^+$ effective mass of the Y_1^0 and Y_2^0 spherical harmonic moments for the angular distribution of the \bar{K}^- relative to the beam direction as axis in the $K^-\pi^+$ rest frame for events fitting the reaction $K^-\rho \rightarrow K^-\pi^+\pi^-$.

Fig. 17. This dependence agrees strikingly well with that seen in the $K^+\rho$ data. The Deck mechanism, illustrated in Fig. 18, provides an explanation for this similarity due to the presence of a $K\pi$ vertex. In fact, recent interpretation of the duality hypothesis indicates that such a diagram could describe the Q region in some average sense and such a description is not inconsistent with an explanation involving $K\pi\pi$ resonances.²² With this in mind, it is noteworthy to consider the quantum numbers of the $K\pi\pi$ system associated with the s -wave $K\pi$ system responsible for the forward asymmetry. The dominant mode in the Q region is a $1^+ \bar{K}^*\pi$ system in a relative s wave. In order to produce an s -wave- p -wave interference, the π^- must also be in an s wave relative to the s -wave $K\pi$ system, resulting in a $0^- K\pi\pi$ state.

In summary, we conclude that our data are consistent with a diffractively produced $J^P=1^+$ $K\pi\pi$ system with a strong p -wave $K\pi$ final-state interaction. An admixture of a $J^P=0^- K\pi\pi$ system²³ with an s -wave $K\pi$ final-state interaction is also required.

D. $\pi^+\pi^-$ System

The $\pi^+\pi^-$ mass spectrum for events belonging to reaction (1.1) is shown in Fig. 19. There is an enhancement of events with a $\pi^+\pi^-$ mass between 600 and 800 MeV. The Dalitz plots for separate intervals of $K^-\pi^+\pi^-$ mass, in Fig. 20, show that this $\pi^+\pi^-$ enhancement is associated with the $\bar{K}^*(890)$ mass band. The fraction of $K\rho$ in the Q region is found to be $\sim 10\%$. This is discussed in Sec. IV.

IV. DOUBLE-REGGE-POLE MODEL

A Reggeized version of the diffraction-dissociation model has recently claimed considerable success in describing the main features of the threshold $K^*\pi$ enhancement produced in $K^\pm\rho$ interactions.²⁴ The low-mass $K\pi\pi$ system produced coherently in $K^-\rho$ interactions shows the same diffractive features as in $K^\pm\rho$

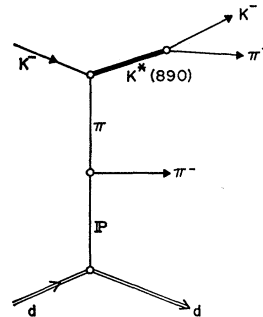


FIG. 18. Diagram representing the double-Regge-pole model used to fit the data from reaction (1.1).

²² G. F. Chew and A. Pignotti, Phys. Rev. Letters **20**, 1078 (1968).

²³ A similar observation has been made for the $\rho\pi$ system; see A. M. Cnops *et al.*, Phys. Rev. Letters **21**, 1609 (1968).

²⁴ J. Andrews *et al.*, Phys. Rev. Letters **22**, 731 (1969); C. Chien *et al.*, University of California, Los Angeles, Report No. UCLA-1031 (unpublished); M. L. Ioffredo *et al.*, Phys. Rev. Letters **21**, 1212 (1968).

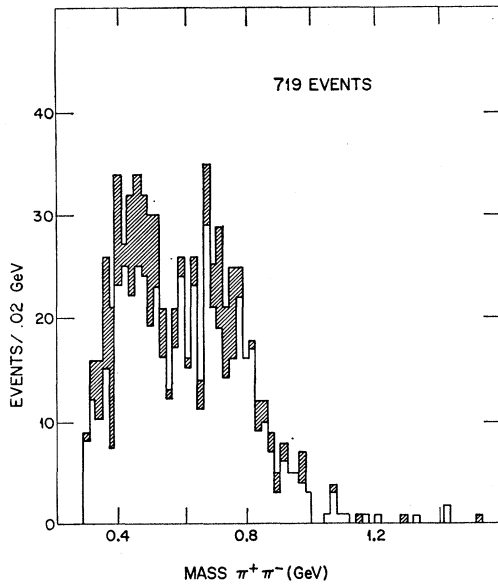


FIG. 19. Effective mass distribution of the $\pi^+\pi^-$ combination for the reaction $K^-d \rightarrow K^-d\pi^+\pi^-$. Events with a $d\pi^-$ mass less than 2.28 GeV are shown shaded.

interactions. The constant cross section for the reaction $K^-d \rightarrow Q^-d$ as a function of beam momentum¹⁸ and the observed alignment of the Q suggests that the Q is produced diffractively. The similarity of the mass dependence of the $K\pi$ decay moments in these data with that observed in the 7.3-GeV/c $K^+p \rightarrow K^+\pi^-\Delta^{++}$ data suggests that the multiperipheral diagram shown in Fig. 18 might successfully describe the production of the Q . We have considered only this diagram in our analysis.

The square of the matrix element for the double-

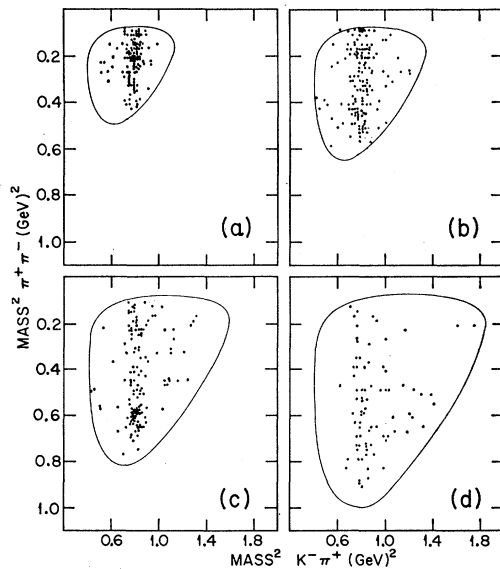


FIG. 20. Dalitz plots for the $K^-\pi^+\pi^-$ system for various intervals of $K^-\pi^+\pi^-$ mass.

Regge-pole-exchange model is given by

$$\sum |M|^2 \propto q^2 (\pi\alpha')^2 \frac{e^{\lambda t_{dd}}}{1 - \cos\pi\alpha_\pi} (s_1 \cdots) \left(\frac{s_2 \cdots}{s_0} \right)^{2\alpha_\pi}, \quad (4.1)$$

where

$$q^2 = [m_{K^-\pi^+}{}^2 - (m_K + m_\pi)^2][m_{K^-\pi^+}{}^2 - (m_K - m_\pi)^2] / 4m_{K^-\pi^+}{}^2,$$

$$s_1 \cdots = [s_{\pi^-d} - (m_d + m_\pi)^2][s_{\pi^-d} - (m_d - m_\pi)^2],$$

$$s_2 \cdots = s_{K\pi\pi} - t_{dd} - m_K^2 - (m_{K^-\pi^+}{}^2 - m_K^2 - t_{KK^*})$$

$$\times (t_{dd} + t_{KK^*} - m_\pi^2) / 2t_{KK^*},$$

$$\alpha_\pi = \alpha' (t_{KK^*} - m_\pi^2).$$

This form was used in a Monte Carlo calculation²⁵ to obtain the predictions of the double-Regge-pole model.¹² We use a value for Λ of 25 GeV⁻² and took α_π' and s_0

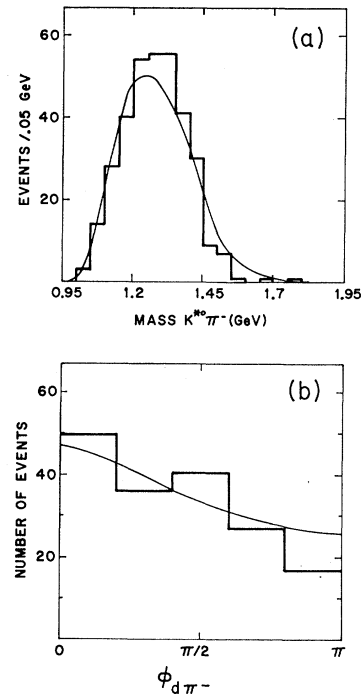


FIG. 21. (a) Distribution in effective mass of the $\bar{K}^*\pi^-$ combination. (b) Treiman-Yang angle distribution at the π^-d vertex with the definition

$$\cos\Phi = \frac{\mathbf{d}_{\text{targ}} \times \mathbf{K}_{\text{inc}}}{|\mathbf{d}_{\text{targ}} \times \mathbf{K}_{\text{inc}}|} \cdot \frac{\mathbf{d}_{\text{targ}} \times \mathbf{d}}{|\mathbf{d}_{\text{targ}} \times \mathbf{d}|}.$$

The solid curve in both cases represents the prediction of the double-Regge-pole model normalized to the observed number of events. Both the data and the model prediction contain the cuts; $(\text{mass})^2(d\pi^-) > 6 \text{ GeV}^2$, $|t_{dd}| > 0.02 (\text{GeV}/c)^2$, and $|t_{KK^*}| < 1.0 (\text{GeV}/c)^2$.

²⁵ A Monte Carlo program based on the LRL subroutine GENEVE was used to generate events of the type $K^-d \rightarrow K^-\pi^+\pi^-d$, which were then weighted according to the double-Regge-pole matrix element. The $\bar{K}^*\pi^-$ mass spectrum was generated with the shape of a Breit-Wigner centered at 890 MeV, with a width of 50 MeV. The decay angular distribution of the $K\pi$ system with respect to the beam direction was chosen using the experimentally determined moments as a function of $K\pi$ mass for the reaction $K^+p \rightarrow K^+\pi^-\Delta^{++}$; see Ref. 10.

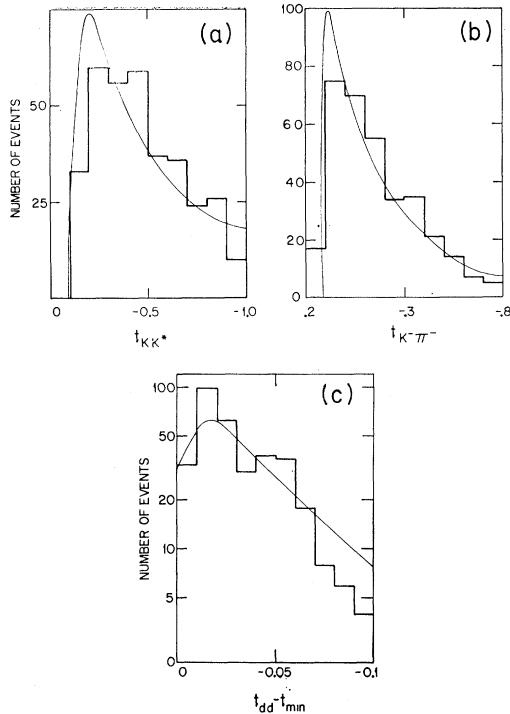


FIG. 22. (a) Distribution in the four-momentum transfer squared between the incident K^- and outgoing $\bar{K}^*(890)$. The curve is obtained using the double-Regge-pole model. (b) Similar distribution for the incident K^- and outgoing π^- . (c) Similar distribution for the incident and outgoing deuteron.

to be 1.2 and 0.8 GeV^2 , respectively, as suggested by the best fits to other processes analyzed using the double-Regge-pole model.²⁴

In comparing the model with the data, the same cuts were used in both. We chose $|t_{KK^*}| < 1.0 (\text{GeV}/c)^2$ and $s_{\pi^-d} > 6.0 \text{ GeV}^2$, in accordance with the region of applicability of the Regge-pole model.¹² A cut requiring $|t_{dd}| > 0.02 (\text{GeV}/c)^2$ was made in order to remove events from the generated sample, since such events are known to have a scanning bias and were likely to

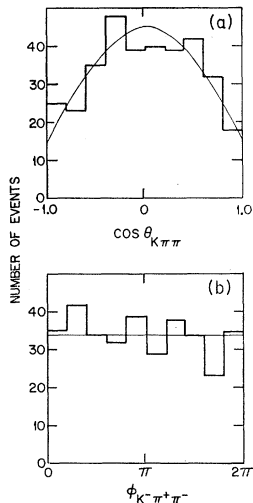


FIG. 23. Polar and azimuthal angular distributions for the $K\pi\pi$ -decay plane normal distribution as defined in Fig. 13, for $\bar{K}^*\pi$ events in the Q region. The solid curve shows the prediction of the double-Regge-pole model.

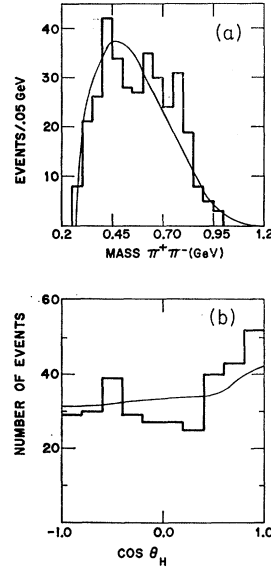


FIG. 24. (a) Effective mass distribution of the $\pi^+\pi^-$ combination for the reaction $K^-d \rightarrow \bar{K}^*(890)\pi^-d$ compared with the double-Regge-pole model prediction shown as a solid curve. (b) The helicity angle distribution for the $\bar{K}^*(890)$ decay defined in Fig. 15, using events from the reaction $K^-d \rightarrow \bar{K}^*\pi^-d$, compared with the double-Regge-pole model prediction shown as a solid curve.

have been lost in the data as three prongs. In Figs. 21–25 the distributions generated by the model for various kinematic quantities are shown as curves and compared with the actual data by normalizing to the observed number of events.

As previously pointed out,¹² the $K\pi\pi$ mass is linearly related to the Treiman-Yang angle at the diffractive vertex. Both distributions are quite well described by the model as shown in Fig. 21. The calculated $K\pi\pi$ mass distribution peaks at the right mass but is slightly too broad, which is characteristic of most double-Regge-pole model fits to the Q enhancement. The $d\pi^-$ Treiman-Yang decay angular distribution shows an anisotropy for both the generated and actual events. This latter prediction is in contrast to the isotropy obtained using a simple OPE model.¹² It is also well known that the OPE model predicts a $K^-\pi^+\pi^-$ mass spectrum which is too broad, this feature being more pronounced as the incident beam momentum is increased.

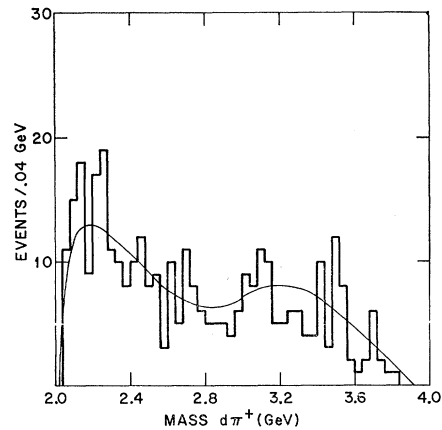


FIG. 25. Effective mass distribution of the π^+d combination compared with the double-Regge-pole model prediction represented by the solid line.

Momentum-transfer-squared distributions are shown for three particle combinations in Fig. 22. The t_{KK^*} distribution is well described by the model. The agreement with the $t_{K^- \pi^-}$ distribution is reasonable at large t but there is an apparent disagreement for low values of $t_{K^- \pi^-}$, where the model predicts a larger number of events than actually occur. The distribution of the quantity $t_{dd} - t_{\min}$ again shows reasonable agreement with the model.

The polar and azimuthal distributions of the normal to the decay plane of the $K\pi\pi$ system are seen in Fig. 23, with good agreement between the data and the model. This is a result of the assumption of a dominant $\cos^2\theta$ dependence for the decay angular distribution of the $K^- \pi^+$ system as well as the s -wave $\bar{K}^* \pi$.

The $\pi^+ \pi^-$ mass distribution and the decay angular distribution of the \bar{K}^* helicity angle θ_H are shown in Fig. 24. The $\pi^+ \pi^-$ mass spectrum shows an excess of events in the ρ region above the prediction of the model. An excess of similar magnitude above the isotropic distribution predicted by the model for the helicity angle is seen for $\cos\theta_H$ near 1.0. Ignoring complications due to crossing \bar{K}^* and ρ bands, we estimate the amount of ρ present to be about 10% of the sample.

The $(d\pi^+)$ mass distribution predicted by the model is shown by the solid curve in Fig. 25. The shape of this distribution is seen to be strongly influenced by the reflection of the \bar{K}^{*0} decay, which produces broad enhancements at both low and high masses, particularly the former.

The double-Regge-pole model gives a good fit to the gross characteristics of our data. This in no way excludes the possibility that one or more resonances may occur in the low-mass $\bar{K}^* \pi$ enhancement. According to the duality hypothesis, the t -channel process calculated above could describe the average behavior of perhaps several closely spaced resonances.

V. CONCLUSIONS

We have studied the production and decay characteristics of the Q enhancement produced in the reaction $K^- d \rightarrow K^- \pi^- \pi^+ d$. We find no evidence for mass structure within this enhancement. The spin-parity assignment is found to be mainly $J^P = 1^+$. In agreement with previous experiments which observe K^{*0} production, our data indicate the polar-angle decay distribution with respect to the beam direction to have a marked asymmetry. We further observe the mass dependence of the spherical harmonic moments of the $K^- \pi^+$ decay distribution to be in striking agreement with that observed in the reaction $K^+ \pi^- \rightarrow K^+ \pi^- \Delta^{++}$. An explanation of this asymmetry requires the presence of a $J^P = 0^-$ $K\pi\pi$ system throughout the Q region. The Reggeized Deck model is found to provide an acceptable description of most features of our data.

ACKNOWLEDGMENTS

We thank the operating crews of the ZGS and of the 30-in. bubble chamber for their cooperation, and also our scanning and measuring staff for their careful work.

Experimental Study of the Decay $K_L \rightarrow \pi^0 \pi^0$ and Other Rare Decay Modes*†

M. BANNER,‡ J. W. CRONIN, J. K. LIU,§ AND J. E. PILCHER||
Palmer Physical Laboratory, Princeton University, Princeton, New Jersey 08540
(Received 8 August 1969)

We have measured the branching ratio $\Gamma(K_L \rightarrow 2\pi^0)/\Gamma(K_L \rightarrow 3\pi^0)$ to be $(4.6 \pm 1.1) \times 10^{-3}$. This leads to $\Gamma(K_L \rightarrow 2\pi^0)/\Gamma(K_L \rightarrow \text{all}) = (0.97 \pm 0.23) \times 10^{-3}$ and a CP -violation parameter $|\eta_{00}| = (2.2 \pm 0.3) \times 10^{-3}$. We also report $\Gamma(K_L \rightarrow \gamma\gamma)/\Gamma(K_L \rightarrow \text{all}) = (4.7 \pm 0.6) \times 10^{-4}$, $\Gamma(K_S \rightarrow \gamma\gamma)/\Gamma(K_S \rightarrow \text{all}) < 0.02$ with 90% confidence and $\Gamma(K_L \rightarrow \pi^0\gamma\gamma)/\Gamma(K_L \rightarrow \text{all}) < 2.3 \times 10^{-4}$ with 90% confidence.

I. INTRODUCTION

THE discovery of the decay mode $K_L \rightarrow \pi^+ \pi^-$ has led to extensive experimental study of the neutral- K -meson system.² At present, the experiments

strongly indicate a violation of CP symmetry.³ Extensive efforts to find CP nonconservation and T violation in systems other than the neutral K system

* Work supported by the U. S. Office of Naval Research, under Contract No. N0014-67-A-0151-0001, and by the U. S. Atomic Energy Commission, under Contract No. AT(30-1)-2137. This work also made use of computer facilities supported in part by National Science Foundation Grant Nos. NSF-GJ-34 and NSF-GU-3157.

† Further details on this work appear in the doctoral theses of two of the authors (J. K. L. and J. E. P.), Technical Reports 48 and 49, Elementary Particles Laboratory, Princeton University (unpublished).

‡ On leave from Département de Physique des Particules Elementaires, Centre d'Etudes Nucléaires, Saclay, France.

§ Present address: Stanford Linear Accelerator Center, Stanford, California 94305.

|| Present address: CERN, 1211 Geneva 23, Switzerland.

¹ J. H. Christenson, J. W. Cronin, V. L. Fitch, and R. Turlay, Phys. Rev. Letters **13**, 138 (1964).

² There have been many excellent reviews of the experimental situation for K decay. See, e.g., L. B. Okun and C. Rubbia, in *Proceedings of the International Conference on Elementary Particles, Heidelberg, 1967*, edited by H. Filthuth (North-Holland Publishing Co., Amsterdam, 1968), p. 301.

³ P. K. Kabir, Phys. Rev. Letters **22**, 1018 (1969); P. Darriulat, J. P. Deutsch, K. Kleinknecht, C. Rubbia, and K. Tittel, Phys. Letters **29B**, 132 (1969).